Published in final edited form as:
Biomaterials. 2013 December ; 34(37): 9331–9340. doi:10.1016/j.biomaterials.2013.08.016.

Capillary Morphogenesis in PEG-Collagen Hydrogels

Rahul K. Singh[1], **Dror Seliktar**[2], and **Andrew J. Putnam**[1,*]

[1]Department of Biomedical Engineering, University of Michigan, Ann Arbor, MI 48109, USA

[2]Faculty of Biomedical Engineering, Technion-Israel Institute of Technology, Technion City, Haifa 32000, Israel

Abstract

A wide variety of hydrogels have been explored as 3D culture platforms and for applications in tissue engineering. Hydrogels formed from natural extracellular matrix (ECM) proteins readily support the formation of vasculature *in vitro*, but only a handful of hydrogels composed of synthetic materials have shown anything comparable. This relative lack of synthetic material options has hindered efforts to better understand how ECM cues direct vascularization. We developed a biosynthetic hydrogel consisting of polyethylene glycol diacrylamide conjugated to macromolecular type-I collagen. Through their acrylamide-based cross-links, these materials allow for independent control of physical properties and bulk ligand concentration. These hydrogels exhibited hydrolytic stability, but the collagen component retained its susceptibility to enzymatic remodeling. Photoencapsulation of endothelial cells and fibroblasts within this hydrogel material and their subsequent co-culture led to the formation of capillary vessel-like networks with well-defined hollow lumens. Capillary formation was prevented by inhibiting matrix metalloproteinase (MMP) activity, recapitulating the MMP-dependence of vascularization observed in natural hydrogels. These findings validate the utility of this material platform to decipher how the ECM regulates capillary morphogenesis and to support the formation of vascularized tissue constructs for potential applications in regenerative medicine.

Keywords

Angiogenesis; Endothelial cell; Hydrogel; Collagen; Photopolymerization; Polyethylene Oxide

Introduction

A number of pathologic conditions are characterized by a lack of vascularization and inadequate blood supply to the tissue, often leading to necrosis [1]. Tissue engineering approaches attempt to address this problem by providing a replacement for the diseased tissue and aiding re-vascularization. One such approach combines cells with a suitable extracellular matrix (ECM) in an attempt to recapitulate the native tissue [2, 3]. Previous work has established that natural ECMs of fibrinogen [4] and collagen [5] readily support vascularization, but these protein hydrogels are limited in their range of physical properties.

*Corresponding author: Andrew J. Putnam, Ph.D. Department of Biomedical Engineering, University of Michigan, 2154 Lurie Biomedical Engineering Building, 1101 Beal Ave, Ann Arbor, MI 48109, Phone: (734) 615-1398, Fax: (734) 647-4834, putnam@umich.edu.

These properties are commonly modulated by changing the concentration of the protein, which simultaneously changes the number of ligands available for cell adhesion, the protease sensitivity, and the matrix architecture [6]. Conversely, synthetic ECM can theoretically provide a range of physical properties with independent control over bulk ligand concentration and matrix architecture. However, only a handful of papers have demonstrated the formation of vascular networks within a synthetic gel *in vitro* [7–12], and thus deconstructing the ECM's multivariable instructive role in the process of capillary morphogenesis continues to be a challenge [13].

Prior studies in the literature have demonstrated the migration of cells in PEG hydrogels from EC spheroids [14], EC and FB aggregates [12], and aortic arches [7]. In most cases, these hydrogels were functionalized with RGD, the minimal cell-adhesive binding domain found in fibronectin [7, 9], and included a mechanism for cell-mediated degradation through the incorporation of peptide cross-links sensitive to proteases [7, 12]. These limited instructive cues (combined with the right soluble factors) have been sufficient to support formation of vessel-like networks *in vitro*, but have performed even better at supporting vascularization *in vivo* when combined with protease-mediated release of pro-angiogenic growth factors [14–16]. Adding in additional peptide motifs may improve the vasculogenic potential of these synthetic platforms even further, but the high cost of purchasing or synthesizing purified peptides can be prohibitive for many laboratories. As a complement to these peptide-functionalized materials, hybrid approaches that utilize conjugate chemistry to covalently link synthetic polymers with biologic macromolecules have also been developed. This approach enables the creation of biosynthetic ECMs with the biological properties defined by the protein and microarchitectures by the synthetic polymer. Previous studies have produced biosynthetic hydrogels utilizing synthetic polymers linked to portions of collagen & fibrinogen [17–19], gelatin [10, 20], heparin [21], and hyaluronic acid [11].

We utilized a biosynthetic hydrogel approach in order to investigate the influence of hydrogel physical properties on the formation of capillary networks *in vitro*. The benefit of the biosynthetic approach in this context is that the bulk concentration of native ECM molecules can be held constant while the physical properties can be controlled orthogonally through synthetic crosslinking. Our approach was to conjugate non-denatured collagen to poly(ethylene glycol) diacrylamide (PEGDAm) to produce a macromolecule. We photopolymerized these macromolecules with varying amounts of exogenous PEGDAm to produce cross-linked amorphous hydrogels, and characterized their bulk mechanical and transport properties. We then investigated the ability of these constructs to support co-cultures of endothelial cells and fibroblasts *in vitro*.

Materials & Methods

Cell Culture

Human umbilical vein endothelial cells (EC) were isolated as described previously [22], and cultured in endothelial growth medium (EGM-2, Lonza, Walkersville, MD) at 37°C, 5% CO_2 and used at passage 2. Normal human lung fibroblasts (FB, Lonza) were cultured in DMEM (Invitrogen) supplemented with 10% fetal bovine serum (FBS, Life Technologies) at 37°C, 5% CO_2 and used between passages 9 and 12. Cell types were chosen that had previously been shown to support robust capillary formation *in vitro* [6, 23]. This allows us to control for variability between endothelial and stromal types and to evaluate the performance of our material. For routine culture, medium was changed every other day and cells were harvested at 80% confluence with 0.05% Trypsin EDTA (Life Technologies).

Synthesis of PEG-diacrylamide

Poly(ethylene glycol) was functionalized as described elsewhere [24]. Briefly, poly(ethylene glycol) (20 kDa MW, 100 g, 10 mM -OH) (Fluka, Buchs, Germany) was dried azeotropically against benzene and reacted with triethylamine (4.1 mL, 30 mmol, Acros, Fair Lawn, NJ) and mesyl chloride (2.3 mL, 30 mmol, Acros) overnight under nitrogen at 20°C. The product was precipitated in cold ether (Fisher, Waltham, MA), dried under vacuum and reacted against 25% aqueous ammonia (Acros) for 4 days. After evaporating the ammonia, the pH was adjusted to 13 with 1 N NaOH, and the solution was extracted with dichloromethane (Fisher), concentrated, precipitated, and dried. The resulting poly(ethylene glycol)-di-amine was dialyzed against water and stored at −80°C. For acrylation, 20 mg of the PEG- diamine intermediate was lyophilized and dried azeotropically before addition of dichloromethane, triethylamine (0.41 mL, 3 mmol), and acroyl chloride (0.23 mL, 3 mmol, Aldrich, St. Louis, MO). The reaction proceeded overnight under nitrogen and the product was precipitated and dried. The resulting poly(ethylene glycol)-di-acrylamide (PEGDAm) was dissolved in water, lyophilized and kept at −20°C. Conversion of diols to diacrylamides was confirmed via ^{1}H NMR: (DCCl3) 3.6 ppm (1816 H, PEG), 5.6 ppm (dd, 2 H, CH2=C*H*-CON-), 6.1 ppm, 6.2ppm (dd, 4 H, C*H*2=CH-CON-).

Conjugation of PEGDAm to Collagen & SDS-PAGE

To conjugate PEGDAm to type-I collagen, a modification of a protocol developed by Gonen-Wadmany et al. [17] was used. All steps were performed at 4°C in PBS to prevent denaturing the collagen. Bovine type I collagen (Nutragen, Advanced BioMatrix, San Diego, CA) was diluted to 3 mg/mL in PBS. SATA (N-succinimidyl S-acetylthioacetate, Thermo Scientific, Rockford, IL) was added at 0.075 mg/mg collagen and the reaction proceeded for 24 hours with agitation then purified by dialysis. Thiols were exposed by reaction with 1.8 M hydroxylamine (Acros) and reduced by *tris*(2-carboxyethyl)phosphine, (TCEP, Sigma) then purified by dialysis. Utilizing a Michael's type addition, the product was conjugated to 20 kDa PEGDAm at 4 mg/mg collagen in PBS with 0.15 M triethanolamine and 0.27 mM TCEP at pH 8.3 overnight with agitation then purified by dialysis against PBS through a 50 kDa membrane (Spectrum Labs Rancho Dominguez, CA). The product was aseptically collected and stored at −20°C. Thiols were quantified prior to PEGylation by Ellman's assay and the PEGDAm content determined by dry weight of the final product.

The reaction between PEGDAm and collagen was sampled at 0, 1, 3, 6, 18 hours and the product was reduced in Laemmli buffer before being run in a 10% Tris-Gly polyacrylamide gel (Invitrogen, Carlsbad, CA). Bands were visualized by staining with 0.1% w/v Coomassie blue G250 (Amresco, Solon, OH) and the gel was photographed with an Epson V300 photo scanner.

Rheological Measurements & Hydrogel Degradation

Hydrogels were formulated with PEG-collagen diluted to 2.5 mg/mL with varying amounts of PBS and PEGDAm to achieve the final weight percent of exogenous PEGDAm denoted PC+n%PEG; the photoinitiator Irgacure 2959 (Ciba, Basel Switzerland) was added at a final concentration of 0.6% w/v to form a precursor solution. To assess the kinetics of hydrogel formation, solutions were cured on a 20 mm UV stage in an AR-G2 rheometer (TA Instruments, New Castle, DE) with an oscillation of 1% strain at 1 rad/s with 5 minutes of exposure to 365nm UV light at 2 mW/cm^2.

For bulk mechanical testing, 200 μL of precursor solution was aseptically cast into 8 mm cylinders in a Teflon mold by exposure to UV light at 365 nm, 2 mW/cm^2 for 5 minutes. Hydrogels were transferred to 24-well plates and incubated in PBS + 0.1% Azide at 37°C

for 1, 3, 7, or 14 days. Rheological measurements were taken with an 8 mm parallel plate on a Peltier stage at 37°C under PBS; both surfaces were coated with P800 wet or dry sandpaper (3M, St. Paul, Minnesota) to prevent slip. Gaps were adjusted to accommodate the swollen height of the hydrogels. The storage and loss moduli were averaged from mechanical spectra from 0.1 to 10 rad/s at 1% strain. The wet and dry weights of each gel were recorded, and the supernatant was assayed for total protein with Bradford's Assay. The mass swelling ratio was calculated from the wet (W_w) and dry (W_D) weights of the gels, excluding the mass of PBS salts (W_S), as $(W_w\text{-}W_S)/(W_D\text{-}W_S)$. Bulk mechanical testing of cellularized hydrogels were conducted in a similar manner, but were cultured in EGM-2 instead of PBS.

Dextran Release

The bulk transport properties of the hydrogels were assessed using dextran to simulate the diffusion of macromolecular species [6]. Acellular 100 μL hydrogels were aseptically cast containing 10 μg of 70 kDa Texas red-conjugated dextran (Life Technologies, Carlsbad, CA). Hydrogels of each formulation were placed in 24-well plates with sterile PBS and incubated at 37°C. The supernatant was aseptically collected after 1, 3, 6, 9, 12, 24 and 72 hours and replaced with fresh PBS each time. After 72 hours, gels were digested overnight with 40 IU collagenase (Worthington Biochemical, Lakewood, NJ) in PBS to release any remaining dextran. The supernatants from each time point and from the digested gels were assayed in a Fluoroskan Ascent FL (Thermo Scientific) plate reader at Ex:595/Em:615. Masses were determined by comparison to a standard curve of dextran and appropriate buffer.

Collagenase Digestion

To detect the release of cleaved PEG-collagen, conjugates were labeled with ATTO-390 NHS-ester (Fluka) at 21 μg per 3 mg collagen at 4°C overnight at pH 7.4. The labeled conjugate was used to produce hydrogels of each formulation. Unreacted ATTO-390 was removed by washing the gels for 3 days in PBS. Samples were then transferred to a 1 mL solution of 20 IU collagenase and incubated at 37°C in the dark. Samples of supernatant (0.3 mL) were taken after 0.25, 1, 3, 6, 9, and 24 hours and replaced with fresh collagenase solution. The fluorescence intensity of the samples was measured at Ex: 355 Em: 485. The concentration of dye was determined through the dilution factor and molar extinction coefficient of ATTO-390: 24000 mol^{-1} cm^{-1}.

Cell Encapsulation & Culture

Cells were encapsulated at either 1e6 EC/mL or 1e6 FB/mL for monoculture, or 1e6 EC and 1e6 FB per mL for co-culture conditions. Cells were resuspended in 1 mL of hydrogel precursor solution, divided into 100 μL aliquots, and photopolymerized in 4.7 mm diameter syringe top [25]. To prevent constructs from adhering to the culture surface, 24-well plates were coated with 1% agarose (Denville, Metuchen, NJ). Media were changed after 3 hours and then every other day thereafter. For a subset of experiments, constructs were cultured in EGM-2 containing either 1 mM or 5 mM GM6001 (EMD Chemicals, San Diego, CA) dissolved in DMSO to inhibit MMPs; as a control, constructs were treated with the vehicle alone. GM6001 was replenished with each media change.

Control constructs were prepared with unmodified collagen diluted to 2.5 mg/mL with sterile water and 10x PBS before raising the pH to 7.2 with 0.1 N NaOH. Cell pellets were suspended in the solution and pipetted in 100 μL drops on non-treated tissue culture 24-well plates and cured for 1 hour before addition of media. After two days of culture, collagen hydrogels were transferred to agarose-coated plates.

Cell Viability

Cell viability was assessed after 1 and 3 days in 4.7 mm constructs with a LIVE/DEAD kit (Invitrogen). Fluorescent images were taken with an Olympus IX81 microscope equipped with a 100 W high pressure mercury lamp (Olympus, Center Valley, PA) and Hammamatsu camera (Bridgewater, NJ) and stained cells were counted using the Count Nuclei module of MetaMorph (Molecular Devices, Sunnyvale, CA).

Hydrogel Compaction

After 14 days of co-culture, 4.7 mm hydrogel plugs were transferred to untreated 24-well plates and suspended in PBS before photography with an EPSON perfection V300 photo scanner (Suwa, Japan). The diameters were measured from the digital images using NIH Image J (National Institutes of Health, Bethesda, Maryland). Separately, gels were placed on a glass slide and photographed with a Casio Exilm digital camera (Tokyo, Japan) to illustrate the 3D shape of the gels.

Time-Lapse Imaging of EC Organization

ECs were fluorescently labeled by transduction with a gene encoding mCherry. Phoenix Ampho cells (Orbigen, San Diego, CA) were transfected with a pBMN-mCherry plasmid using Lipofecamine 2000 (Invitrogen). Retroviral containing supernatant was collected, passed through a 0.45 μm filter, and supplemented with 5 μg/mL Polybrene (EMD Millipore, Billerica, MA) before incubation with EC for 12 hours. The media was changed to EGM-2 and cells were cultured for 2 days, passaged once, and frozen until use. Constructs were prepared with mCherry-labeled EC and wild-type FB and allowed to float freely in agarose coated wells and photographed with an Olympus Microscope (Ex:558/Em: 583) *in situ* daily for 14 days. A custom MATLAB script was used to quantify the total network length from the fluorescent images.

Immunofluorescent Staining

Constructs were washed 3x with PBS then fixed overnight in 4% formaldehyde (Sigma) in PBS at 4°C then washed again. Cells were permeablized with TBS + 1% Triton X-100 (TBS-T), rinsed with TBS-T and blocked with 2% bovine serum albumin (Sigma) in TBS-T (AbDil) overnight at 4°C. Constru cts were incubated overnight at 4°C in a monoclonal mouse anti-human CD31 antibody (Dako, Glostrup, Denmark) diluted 1:200 in AbDil. After multiple washes, samples were then incubated overnight at 4°C in AlexaFluor 594 goat anti-mouse antibody (Invitrogen) diluted 1:450 in AbDil. Further washing was performed before counter-staining with DAPI (1:10,000; Sigma) and Oregon Green 488 phalloidin (1:200; Invitrogen) For α-SMA staining, a similar protocol was utilized with a primary mouse monoclonal anti-α-smooth muscle actin antibody (1:200; AbCam, Cambridge, MA). Fluorescent images of the constructs were taken and the network lengths were quantified using the angiogenesis module in Metamorph.

Results

Synthesis of PEG-Collagen

Conversion of PEG diols to diacrylamides was performed with 95% efficiency. Of the unreacted groups, >93% were amines with minimal acrylate formation. For the conjugation (Fig. 1A), incorporation of thiols was measured at 0.23 ± 0.01 mM or 35 thiols per collagen molecule. The final mass of PEGDAm was determined to be 2.52 ± 0.02 mg per mg collagen for a stoichometric ratio of 57:1; the stoichometric difference between thiols and PEGDAm suggests that some unconjugated PEGDAm remains in the final product.

To confirm conjugation, the product was run through a polyacrylamide gel, with Coomassie staining revealing dark bands near 150 kDa that correspond to the α_1 and α_2 chains of collagen (Fig. 1B). Conjugation of PEGDAm to collagen was evident by disappearance of these 150 kDa bands over time coupled with appearance of a smear at higher molecular weights, with the mobility shift evident within 18 hours.

Gel Formation

Exposure of all three formulations of PEG-collagen to UV light was accompanied by an increase in the shear storage modulus (G') indicative of gel formation (Fig. 1C). The complex shear modulus (G', G'') of the PEG-collagen was increased by addition of exogenous PEGDAm, both prior to and following UV photopolymerization. Nevertheless, the increased storage modulus resulting from the photopolymerization were much pronounced in these samples. The rapid increase in storage modulus of PC+0%PEG solutions following photopolymeriation was followed by a volume relaxation [26], making the apparent pre-UV and post-UV moduli not quite significantly different (Fig. 1D). By contrast, the increase in storage modulus was more gradual for the other two formulations, likely owing to an increase in viscosity, and was significantly increased after UV cross-linking in both cases. Following UV cross-linking, each of the three gel formulations' shear storage moduli were significantly different from one another, spanning two orders of magnitude. The shear loss moduli did not show any significant trends, but were an order lower than the corresponding storage moduli indicating extensive crosslinking of the material.

Assessment of Hydrolytic Stability

Hydrogels were stable in buffer without significant changes over time in the wet mass of the gel (Fig. 2A) or the mass swelling ratio (Fig. 2B). The wet masses were significantly different between formulations ($P<0.01$), with increased water content observed with higher PEGDAm content. However, the mass swelling ratios were not significantly different between formulations. Adopting a published approach [27], the mesh size was estimated to be 61 ± 2 nm at day 1 for the three formulations, and no noteworthy changes were observed thereafter. Additionally, the shear storage modulus of the hydrogels (Fig. 2C) were not significantly changed over 14 days for PC+0%PEG and PC+1%PEG, but the modulus of the PC+2%PEG decreased slightly between days 1 and 3 and remained unchanged thereafter. At each day, the shear modulus of the PC+2%PEG gels was significantly larger than the moduli of the PC+0%PEG and PC+1%PEG gels, but the moduli of the swollen PC+0%PEG and PC +1%PEG gels were not significantly different from each other. The protein content of the buffer increased a small yet significant amount ($P < 0.01$) at day 14 (Fig. 2D), indicating a small loss of protein from the gels over time; however, the total amount released accounts for only 0.01% of the hydrogel's original protein content. Collectively, these data suggest the PEG-collagen hydrogels are hydrolytically stable in an inert aqueous environment.

Dextran Release

To characterize the differential ability of the PEG-collagen hydrogel formulations to limit diffusive transport, the cumulative release profiles of fluorescent dextran was assessed for each hydrogel. Data were normalized to the total mass of dextran entrapped, which includes the mass after collagenase digestion. The best-fit lines are first-order exponential approximations of diffusive processes in high porosity hydrogels (Eqn. 1) [28].

$$M = M_0 + (M_f - M_0)[1 - \exp(-K \cdot t)] \quad \text{Eqn. 1}$$

The equation correlated with the data for PC+ 0%, 1%, and 2% PEG with 70 kDa dextran release (Fig. 2E) R^2: (0.9988, 0.9882, 0.9902) respectively. The rate constant, K, was also calculated for all release profiles and a sum-of-squares F-test suggested significant ($P < 0.05$) differences in the release rates (Fig. 2F). Pair-wise Bonferoni comparisons showed that the release rate of 70 kDa dextran from PC+0%PEG gels was significantly greater than the other conditions.

Collagenase Digestion

To characterize the collagenase sensitivity of our materials, fluorescently labeled hydrogels were prepared with ATTO-390 tagged PEG-collagen. Unreacted ATTO-390 was thoroughly removed by PBS washes with negligible fluorescence of the final PBS wash. All formulations were completely digested by collagenase within 24 hours. The cumulative release of ATTO-390 was assumed to be correlated to the amount of released PEG-collagen with a theoretical labeling ratio of 2.7 fluorophores per collagen molecule. The release profiles (Fig. 3A) followed an exponential (Eqn. 1) with R^2 equal to 0.9544, 0.9478, 0.8098 for PC + 0, 1, & 2% PEG respectively. The rate constant for the release of tagged collagen fragments, K, was also determined and, a sum-of-squares F-test suggested significant ($P < 0.01$) differences in the release rates of fluorophore. Subsequent Bonferoni pair-wise comparisons showed that all three rates were significantly different from each other.

Cellular Viability

More than 60% of cells were found to be viable in all constructs after 24 hours (Fig. 3B). Quantification and comparisons between the conditions (Fig. 3C) revealed viability was highest in PC+0%PEG and similar in the others. Both monocultures and the co-culture showed similar trends with the cell type not being a significant ($P > 0.05$) source of variation by 2-way analysis of variance (ANOVA); pairwise comparisons were determined by Bonferroni post-tests. By day three (Fig. 3D), both the cell type and material had a significant influence on viability. The viability of FB was still close to 60%, but the viability of EC had dropped across all conditions with the PC+2%PEG being the worst. Viability was retained best in co-cultures, which were still comparable to their viability after one day.

Bulk Cellular Remodeling & Hydrogel Compaction

Shear storage moduli of the cell-seeded constructs (Fig. 3E) were similar to the acellular constructs. Significant ($P < 0.05$) differences between formulations at each time point were observed. Linear regression revealed no significant trends over time in the PC+0%PEG and PC+2%PEG gels, but for the PC+1%PEG gels, a significant negative trend ($P < 0.05$) was observed over time.

The constructs, which were initially cast as 4.7 mm plugs, all decreased in diameter (Fig. 3F). The PC+0%PEG and PC+1%PEG gels compacted to the same diameter while the collagen gel compacted to a spherule less than 1 mm in diameter. The PC hydrogels retained a cylindrical shape after 14 days in culture with discernible edges. With the exception of the comparison between PC+0%PEG and PC+1%PEG gels, all other comparisons were significant ($P < 0.01$) by one-way ANOVA and Tukey's post-tests.

Capillary Morphogenesis in PEG-Collagen Hydrogels

When ECs and FBs were co-encapsulated within PEG-collagen hydrogels, the labeled EC elongated and migrated within the first few days of culture (Fig. 4A), leading to the formation of capillary-like networks with discernible tubes by day 10 in PC+0%PEG and day 14 in PC+1%PEG. EC in the PC+2%PEG constructs failed to elongate or form multicellular structures. The collagen constructs rapidly formed networks in one day, but the

EC structures began to regress after the construct was detached from the substrate as significant cell-mediated compaction occurred in subsequent days.

Staining of co-cultures in PC+0%PEG and PC+1%PEG revealed organization of CD31+ cells into tube-like structures by day 14 (Fig. 4B). While very few EC were observed in the PC+2%PEG condition, elongated FB were found throughout the constructs. Further, α-SMA staining revealed cells positive for the marker across all three conditions (Fig. 4C). Quantification of network lengths (Fig. 4D) were found to be significantly ($P < 0.05$) lower in the PC+2%PEG condition, but not significantly different between the PC+0%PEG and PC+1%PEG by a one way ANOVA with Bonferroni post-tests. Confocal z-stacks taken at higher magnification revealed that the CD31+ capillary-like structures possess hollow lumens in the PC+1%PEG condition (Fig. 4E).

MMP Inhibition

Supplementation of culture medium with a broad-spectrum MMP inhibitor, GM6001, prevented endothelial invasion and subsequent organization within the material (Fig. 5A). Quantification of total network lengths revealed significant increases in total network length in cultures treated with 1 μM GM6001 (relative to those treated with DMSO vehicle) treatment across all PC material formulations (Fig. 5B). Further assessment of the mean segment length revealed a dose-dependent decrease across the PC conditions (Fig. 5C). Thus, low doses of GM6001 caused the EC to produce more numerous, yet, shorter tubes in PC+0%PEG and PC+1%PEG hydrogels. EC organization was not observed in the PC +2%PEG gels to an appreciable extent.

Discussion

In this study, we have demonstrated that capillary morphogenesis can be recapitulated *in vitro* in a PEG-based hydrogel by adopting a biosynthetic approach that presents native collagen macromolecules and has permissive mechanical and transport properties. Endothelial cell organization within this biosynthetic hydrogel system was dependent on the degree of crosslinking. By utilizing inert PEGDAm crosslinks, the physical properties of the gels were independently changed without altering the concentration of bioactive sites. Large numbers of immature capillaries formed in the weakly crosslinked gels, while fewer, more mature capillaries formed in the intermediate gels; no capillaries were observed in the most highly crosslinked gels.

At the heart of our approach is a conjugate of PEGdiacrylamide and collagen, which rapidly photopolymerizes into a hydrogel that is hydrolytically stable. The resistance to hydrolysis arises from the amide having a less detrimental effect on the thioether of the Michael's adduct than an ester that results from the more typical linkage to PEGdiacrylate [24, 29]. An earlier approach of making a similar conjugate relied on denaturing buffers to solubilize collagen [17]. We found that the reaction could be accomplished under conditions that preserve the native conformation of the collagen macromolecules. We hypothesize that maintaining the triple-helical structure of the collagen macromolecules provides a native presentation of peptide sequences preserving binding sites for integrins, growth factors, and enzymes [30]. The synthetic modification allows for hydrogels to form by brief exposure to low-power long-wave UV light, forming gels much faster than unmodified collagen. Further, the rapid dissolution of the gels in collagenase demonstrates that the collagen macromolecules play a central role in stabilizing the structure. Thus, the microstructure of the gel is expected to be similar to that of other PEG-based hydrogels; wherein, it is composed of randomly dispersed collagen macromolecules immobilized by PEGDAm crosslinks with increasing amounts of PEGDAm predominantly producing longer crosslinks.

This amorphous PEG-collagen material is in direct contrast to the fibrillar nature of unmodified collagen gels [31].

While the swelling ratios provide rough approximations of mesh size, they could not discriminate between the three formulations owing to their low polymer content. Instead, we utilized dextran release since it provides a more direct assessment of the transport properties than mesh size estimates. The 70 kDa dextran released rapidly in the PC+0%PEG formulation but more slowly in the others, thus indicating that the larger molecules could be entrapped in the PEG-Collagen network as the cross-linking density is increased. Because both the PC+0%PEG and PC+1%PEG gels were comparably able to support capillary formation despite significant differences in their abilities to support diffusive transport, the transport of large molecules appears not to be the factor limiting capillary formation in this system.

Viability of encapsulated cells after 24 hours revealed that most cells survive the photoencapsulation process with monocultures and co-cultures being similarly viable. Cellular responses to the material and culture environment were more apparent after 72 hours. The EC monocultures exhibited the worst viability, but viability was greater for FB and co-cultures. The higher viability of some co-cultures may be due to FB aiding EC survival, as reported by others [32]. Interestingly, the PC+2%PEG gels showed the worst EC viability, but the viability of FB was not abnormal. This differential response of the two cell types may reflect preferences for different ECM stiffness ranges. Compared to the high viabilities (>80%) typically published in cell encapsulation studies [9], the viabilities here are fairly low, even in the pure collagen hydrogels. We attribute these differences to the high cell densities and the fact that constructs were formed in the presence of PBS rather than culture medium.

In the presence of cells, the PEG-collagen gels partially retained their different mechanical properties over extended culture periods, with the shear storage moduli of the PC+2%PEG gels being significantly different than the other two material formulations at all time points tested. However, the differences between the PC+0%PEG and the PC+1%PEG gels were not significant and were in fact quite similar after 14 days of culture, suggesting that the cells remodel both materials to have similar mechanical properties. Minimal compaction of the PC+2%PEG hydrogels was observed, but the compaction of the PC+0%PEG and PC +1%PEG formulations was similar. In contrast, the shear storage modulus of collagen gels [33] is similar to that of the PC+0% PEG, but the collagen gels undergo the highest degree of compaction. These observations suggest that the degree of compaction may be governed by some other criteria than gel's bulk modulus. Other studies have demonstrated that endothelins secreted by EC in collagen gels are responsible for inducing a contractile phenotype in FB [34]. The PC+2%PEG gels do not support EC culture; it follows that the FB are not receiving cues to compact the gels. Interestingly, when constructs are cultured on tissue-culture treated plates, instead of agarose, EC colonize the culture surface. In these conditions, all gel formulations compact and support capillary formation (data not shown). This suggests that the PC+2%PEG gels are not too stiff to be compacted by fibroblasts, rather, it is the EC which modulate FB compaction of the gels.

Endothelial cells organized into networks in both PC+0%PEG and PC+1%PEG formulations. Confocal imaging of the EC networks in PC+0%PEG gels revealed multinucleated EC tube structures. In the PC+1%PEG gels, these tubes were more pronounced and displayed clear lumenal expansion to form capillaries. Networks in PC +0%PEG networks consisted of a larger number of short structures, while the ECs in the PC +1%PEG gels formed fewer but longer structures. These qualitative differences suggest that increased matrix crosslinking affects capillary morphogenesis. This finding is consistent

with a recent study showing that lumen formation in EC-FB co-cultures requires crosslinking of cell-secreted ECM components [32], and suggests the existence of an optimal matrix mechanical environment to support endothelial morphogenesis and maturation. Furthermore, we showed that inhibition of MMPs prevented capillary formation in the PEG-collagen gels, recapitulating the requirement for enzymatic remodeling for the formation of vascular networks in natural materials [35].

In the PC+0%PEG and PC+1%PEG hydrogels, discernible multicellular networks formed on day 10, in contrast to the rapid formation of networks in mechanically anchored collagen gels within one day. However, these EC networks rapidly regressed after the collagen gels were detached from their substrate and placed on agarose. In the PC gels, the large number of PEGDAm crosslinked per collagen molecule stabilize the hydrogels against compaction by slowing the rate of network formation. Relative to unmodified collagen hydrogels and their fibrillar architecture, the amorphous structure and highly-crosslinked nature of the PC gels requires cleavage of a larger number of collagen molecules to create the physical space in the matrix necessary for tubulogenesis. Despite the slower rate of morphogenesis *in vitro*, the benefit of increased mechanical stability may translate to capillary stability *in vivo,* since constructs may not be immediately anchored to the surrounding tissue upon injection or implantation.

Conclusion

We developed a biosynthetic hydrogel that exhibited proteolytic susceptibility coupled with hydrolytic stability, and demonstrated the ability of this material to support and sustain capillary morphogenesis *in vitro*. The physical properties of these hydrogels could be altered by increasing the cross-linking using exogenous PEGDAm, and our data showed that co-encapsulation of EC and FB within these hydrogels yielded mature capillaries with well-defined lumens in hydrogel formulations with up to 1% exogenous PEGDAm. Organization of EC in these hydrogels could be prevented by inhibition of MMP activity, recapitulating the necessity of these proteases for capillary formation observed in native collagen hydrogels. Collectively, these findings demonstrate the utility of this tractable material platform for the assembly of vascularized tissue constructs *in vitro*. Further application of this material platform as a tool to dissect the mechanisms by which the ECM governs vascularization. Further application of this material platform as a tool to dissect the mechanisms by which the ECM governs vascularization may inspire new therapeutic approaches for the treatment of various ischemic diseases.

Acknowledgments

This work was partially supported by grants from the US-Israel Binational Science Foundation (Award #2007366) and the National Institutes of Health (R01-HL085339). RKS was partially supported by a pre-doctoral fellowship from the NIH (NIDCR)-funded Tissue Engineering and Regeneration training program (T32-DE007057) at the University of Michigan.

References

1. Simons M, Ware JA. Therapeutic angiogenesis in cardiovascular disease. Nat Rev Drug Discov. 2003; 2:863–72. [PubMed: 14668807]
2. Losordo DW, Dimmeler S. Therapeutic angiogenesis and vasculogenesis for ischemic disease: part II: cell-based therapies. Circulation. 2004; 109:2692–7. [PubMed: 15184293]
3. Phelps EA, Garcia AJ. Update on therapeutic vascularization strategies. Regen Med. 2008; 4:65–80. [PubMed: 19105617]
4. Tonnesen MG, Feng X, Clark RAF. Angiogenesis in wound healing. J Investig Dermatol Symp Proc. 2000; 5:40–6.

5. Koh, W.; Stratman, AN.; Sacharidou, A.; Davis, GE. In vtro three dimensional collagen matrix models of endothelial lumen formation during vasculogenesis and angiogenesis. In: David, AC., editor. Methods in Enzymology. Academic Press; 2008. p. 83-101.
6. Ghajar CM, Chen X, Harris JW, Suresh V, Hughes CCW, Jeon NL, et al. The effect of matrix density on the regulation of 3-D capillary morphogenesis. Biophys J. 2008; 94:1930–41. [PubMed: 17993494]
7. Miller JS, Shen CJ, Legant WR, Baranski JD, Blakely BL, Chen CS. Bioactive hydrogels made from step-growth derived PEG–peptide macromers. Biomaterials. 2010; 31:3736–43. [PubMed: 20138664]
8. Miller JS, Stevens KR, Yang MT, Baker BM, Nguyen D-HT, Cohen DM, et al. Rapid casting of patterned vascular networks for perfusable engineered three-dimensional tissues. Nat Mater. 2012; 11:768–74. [PubMed: 22751181]
9. Moon JJ, Saik JE, Poché RA, Leslie-Barbick JE, Lee S-H, Smith AA, et al. Biomimetic hydrogels with pro-angiogenic properties. Biomaterials. 2010; 31:3840–7. [PubMed: 20185173]
10. Chen Y-C, Lin R-Z, Qi H, Yang Y, Bae H, Melero-Martin JM, et al. Functional human vascular network generated in photocrosslinkable gelatin methacrylate hydrogels. Adv Funct Mater. 2012; 22:2027–39. [PubMed: 22907987]
11. Hanjaya-Putra D, Wong KT, Hirotsu K, Khetan S, Burdick JA, Gerecht S. Spatial control of cell-mediated degradation to regulate vasculogenesis and angiogenesis in hyaluronan hydrogels. Biomaterials. 2012; 33:6123–31. [PubMed: 22672833]
12. Turturro MV, Christenson MC, Larson JC, Young DA, Brey EM, Papavasiliou G. MMP-sensitive PEG diacrylate hydrogels with spatial variations in matrix properties stimulate directional vascular sprout formation. PLoS One. 2013; 8:e58897. [PubMed: 23554954]
13. Lutolf MP, Hubbell JA. Synthetic biomaterials as instructive extracellular microenvironments for morphogenesis in tissue engineering. Nat Biotechnol. 2005; 23:47–55. [PubMed: 15637621]
14. Zisch AH, Lutolf MP, Ehrbar M, Raeber GP, Rizzi SC, Davies N, et al. Cell-demanded release of VEGF from synthetic, biointeractive cell-ingrowth matrices for vascularized tissue growth. FASEB J. 2003; 17:2260–2. [PubMed: 14563693]
15. Chwalek K, Levental KR, Tsurkan MV, Zieris A, Freudenberg U, Werner C. Two-tier hydrogel degradation to boost endothelial cell morphogenesis. Biomaterials. 2011; 32:9649–57. [PubMed: 21937106]
16. Phelps EA, Landázuri N, Thulé PM, Taylor WR, García AJ. Bioartificial matrices for therapeutic vascularization. Proc Natl Acad Sci U S A. 2009; 107:3323–8. [PubMed: 20080569]
17. Gonen-Wadmany M, Oss-Ronen L, Seliktar D. Protein–polymer conjugates for forming photopolymerizable biomimetic hydrogels for tissue engineering. Biomaterials. 2007; 28:3876–86. [PubMed: 17576008]
18. Martino MM, Briquez PS, Ranga A, Lutolf MP, Hubbell JA. Heparin-binding domain of fibrin(ogen) binds growth factors and promotes tissue repair when incorporated within a synthetic matrix. Proc Natl Acad Sci U S A. 2013; 110:4563–8. [PubMed: 23487783]
19. Lee HJ, Lee J-S, Chansakul T, Yu C, Elisseeff JH, Yu SM. Collagen mimetic peptide-conjugated photopolymerizable PEG hydrogel. Biomaterials. 2006; 27:5268–76. [PubMed: 16797067]
20. Fu Y, Xu K, Zheng X, Giacomin AJ, Mix AW, Kao WJ. 3D cell entrapment in crosslinked thiolated gelatin-poly(ethylene glycol) diacrylate hydrogels. Biomaterials. 2012; 33:48–58. [PubMed: 21955690]
21. Benoit DSW, Durney AR, Anseth KS. The effect of heparin-functionalized PEG hydrogels on three-dimensional human mesenchymal stem cell osteogenic differentiation. Biomaterials. 2007; 28:66–77. [PubMed: 16963119]
22. Griffith CK, Miller C, Sainson RC, Calvert JW, Jeon NL, Hughes CC, et al. Diffusion limits of an in vitro thick prevascularized tissue. Tissue Eng. 2005; 11:257–66. [PubMed: 15738680]
23. Kniazeva E, Putnam AJ. Endothelial cell traction and ECM density influence both capillary morphogenesis and maintenance in 3-D. Am J Physiol Cell Physiol. 2009; 297:C179–87. [PubMed: 19439531]

24. Elbert DL, Hubbell JA. Conjugate addition reactions combined with free-radical cross-lnking for the design of materials for tissue engineering. Biomacromolecules. 2001; 2:430–41. [PubMed: 11749203]
25. Khetan S, Burdick J. Cellular encapsulation in 3D hydrogels for tissue engineering. J Vis Exp. 2009:e1590.
26. Anseth KS, Bowman CN, Peppas NA. Polymerization kinetics and volume relaxation behavior of photopolymerized multifunctional monomers producing highly crosslinked networks. J Polym Sci A Polym Chem. 1994; 32:139–47.
27. Canal T, Peppas NA. Correlation between mesh size and equilibrium degree of swelling of polymeric networks. J Biomed Mater Res. 1989; 23:1183–93. [PubMed: 2808463]
28. Patil NS, Dordick JS, Rethwisch DG. Macroporous poly(sucrose acrylate) hydrogel for controlled release of macromolecules. Biomaterials. 1996; 17:2343–50. [PubMed: 8982474]
29. Browning MB, Cosgriff-Hernandez E. Development of a biostable replacement for PEGDA hydrogels. Biomacromolecules. 2012; 13:779–86. [PubMed: 22324325]
30. Brodsky, B.; Persikov, AV. Molecular structure of the collagen triple helix. In: David, ADP.; John, MS., editors. Adv Protein Chem. Academic Press; 2005. p. 301-39.
31. Seliktar D. Designing cell-compatible hydrogels for biomedical applications. Science. 2012; 336:1124–8. [PubMed: 22654050]
32. Newman AC, Nakatsu MN, Chou W, Gershon PD, Hughes CCW. The requirement for fibroblasts in angiogenesis: fibroblast-derived matrix proteins are essential for endothelial cell lumen formation. Mol Biol Cell. 2011; 22:3791–800. [PubMed: 21865599]
33. Raub CB, Suresh V, Krasieva T, Lyubovitsky J, Mih JD, Putnam AJ, et al. Noninvasive assessment of collagen gel microstructure and mechanics using multiphoton microscopy. Biophys J. 2007; 92:2212–22. [PubMed: 17172303]
34. Guidry C, Hook M. Endothelins produced by endothelial cells promote collagen gel contraction by fibroblasts. J Cell Biol. 1991; 115:873–80. [PubMed: 1918166]
35. Chun T-H, Sabeh F, Ota I, Murphy H, McDonagh KT, Holmbeck K, et al. MT1-MMP–dependent neovessel formation within the confines of the three-dimensional extracellular matrix. J Cell Biol. 2004; 167:757–67. [PubMed: 15545316]

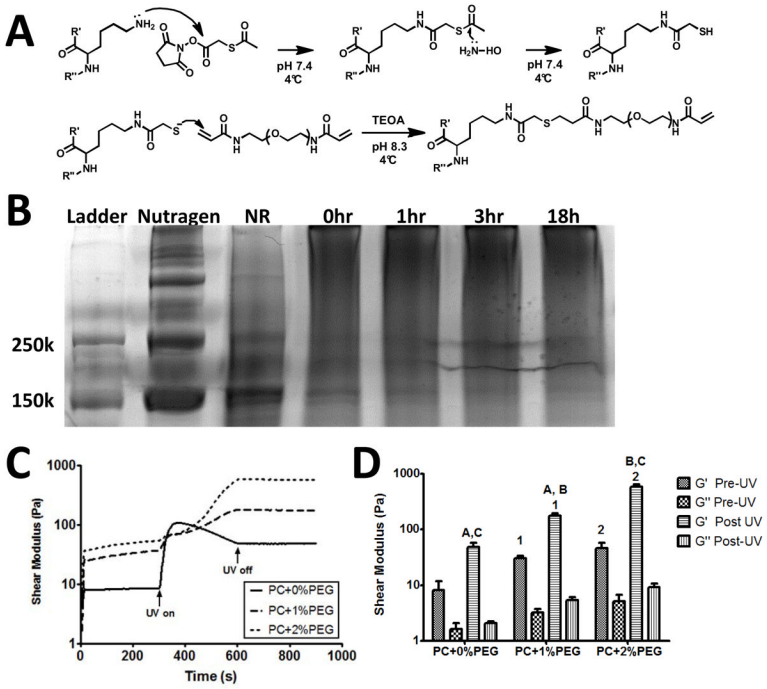

Figure 1. Hydrogels were prepared from PEGylated collagen and subsequent photopolymerization

A) Collagen was modified utilizing SATA to incorporate free thiols, which then reacted with PEGDAm via Michael's type addition to form a PEG-collagen conjugate. B) Formation of this conjugate was evident from the mobility shift during the reaction. The Nutragen and thiolated collagen product (NR) displayed bands near 150 kDa, while under alkaline conditions (0h) the bands disappeared and a high molecular weight smear appeared corresponding to PEGDAm-collagen adducts (18h). C) Subsequent exposure of conjugates (with photoinitiator and varying wt% PEGDAm) to UV light in a parallel plate rheometer led to rapid increases in shear modulus and gel formation. While the crosslinking rate slowed with addition of exogenous PEGDAm, all formulations set within the 5 minutes of UV exposure. D) Comparisons of the shear moduli before and after UV exposure revealed that the final shear storage modulus (G') of each formulation was significantly different from each other; the loss moduli (G'') did not differ significantly. Matched symbols denote $P < 0.01$ (n=3).

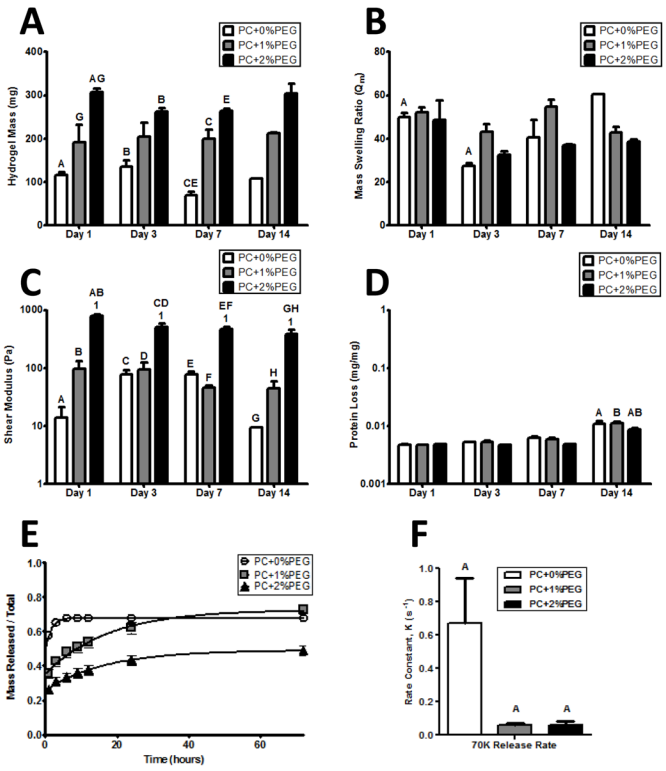

Figure 2. The physical properties of hydrogel formulations are stable in the absence of cells and can be tuned by exogenous PEGDAm incorporation

A) Wet masses of swollen hydrogels of each formulation demonstrated a significantly increased degree of swelling with increasing PEG content. The masses of the gels were stable and did not significantly change over time. B) The mass swelling ratio was also stable and did not show any significant trends with neither the gel formulation nor time in buffer significantly contributing to the variance. C) The shear moduli of the PC+0% & 1% PEG gels did not change over time while the PC+2%PEG showed a slight decrease after day 1. At each day, the shear modulus of the PC+2%PEG gels was significantly different from the PC +0% & 1% PEG gels. D) Protein release from the hydrogels was not significant until day 14 when a negligible amount (0.01% w/w) was detected form all gel formulations. For panels A–D, significance was determined by 2-way ANOVA and Bonferroni post-tests with $p < 0.05$ and denoted by matched symbols on the graphs. To assess the bulk transport properties of the gels, release of encapsulated 70 kDa dextran (E) was monitored and the rate constants were compared (F) with a significantly higher rate for PC+0%PEG and comparable between the other two formulations.

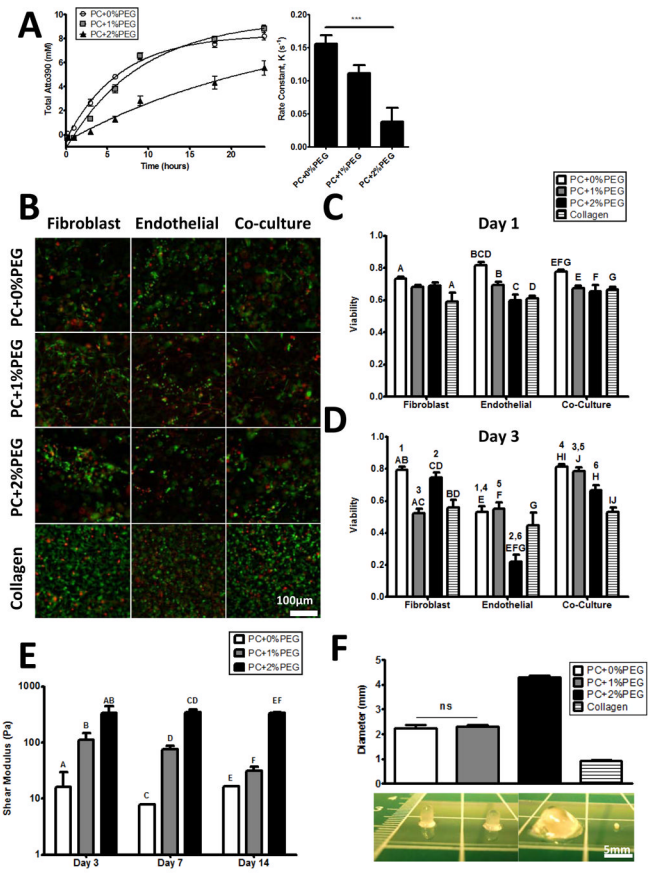

Figure 3. Enzymatic and cellular remodeling of hydrogels proceeds *in vitro*

A) Fluorescently labeled hydrogels were digested in a collagenase solution and release of the fluorophore followed an exponential with the release rate being significantly ($P < 0.01$) different across all conditions. B) A fluorescent assay for viability (green cells are live and red cells are dead) revealed that > 60% of cells are viable after 24 hours in culture (C) with similar viability for all cell types, and only the PC+0%PEG being significantly higher. D) By 72 hours, the viability was influenced by cell type and material with EC-only being the worst. Viability of co-cultures were comparable to the earlier time point.. E) Shear moduli of the hydrogels were significantly different for each formulation at each time point. There were no significant trends over time in the shear moduli of the PC+0%PEG or the PC +2%PEG conditions, but a slight downward trend was observed in the shear modulus of the PC+1%PEG condition. For panels C, D, and E, significant comparisons are indicated on the graphs with matched symbols ($P < 0.05$). F) Constructs were cast as plugs with an initial diameter of 4.7 mm and measured again after 14 days of culture. The diameters significantly decreased with all being different ($P < 0.01$) unless otherwise noted (ns).

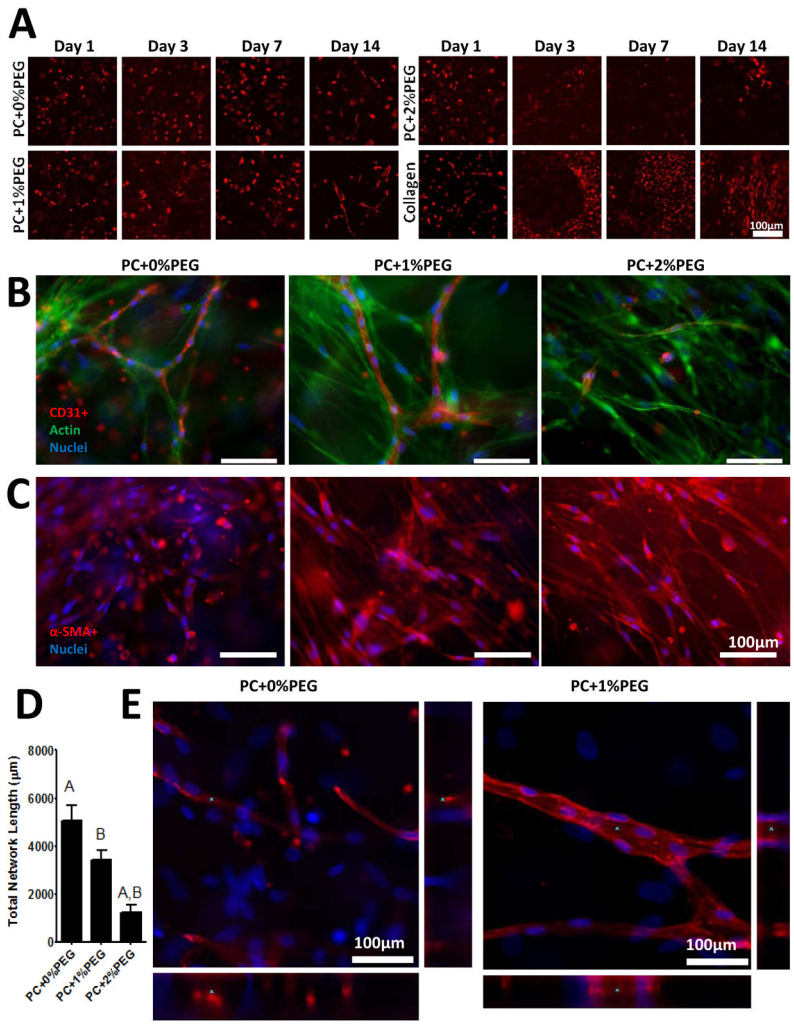

Figure 4. Capillary formation was observed in PEG-collagen hydrogels

A) Constructs prepared with mCherry labeled EC revealed the kinetics of morphogenesis in PC+0%PEG and PC+1%PEG gels. There was little evidence of network formation in PC +2%PEG gels due to the limited survival of EC in those gels. While EC formed networks in 1 day in anchored collagen constructs, detachment of the constructs from the culture surface led to rapid compaction and regression of EC networks. B) Immunofluorescent staining of constructs prepared with wild type EC on day 14 revealed capillary networks in PC+0%PEG and PC+1% PEG (red are CD31+ cells, green is actin, and blue are nuclei). C) Fibroblasts were found to express α-SMA in all three formulations and adopted an elongated morphology in the more crosslinked gels (red are α-SMA+ and blue are nuclei). D) Quantification of total network lengths in the stained images reveled significantly reduced network formation in PC+2%PEG gels with no significant differences between the lengths of PC+0%PEG and PC+1%PEG gels observed. Matched symbols denote significance ($P < 0.01$). E) Confocal stacks of the EC structures in PC+0%PEG (left) and PC+1%PEG (right) revealed lumenal expansion in the PC+1%PEG material (red are α-SMA+ and blue are nuclei). Asterisks (*) on the xy, xz (bottom), and yz (right) panels of each image denote the same region of interest.

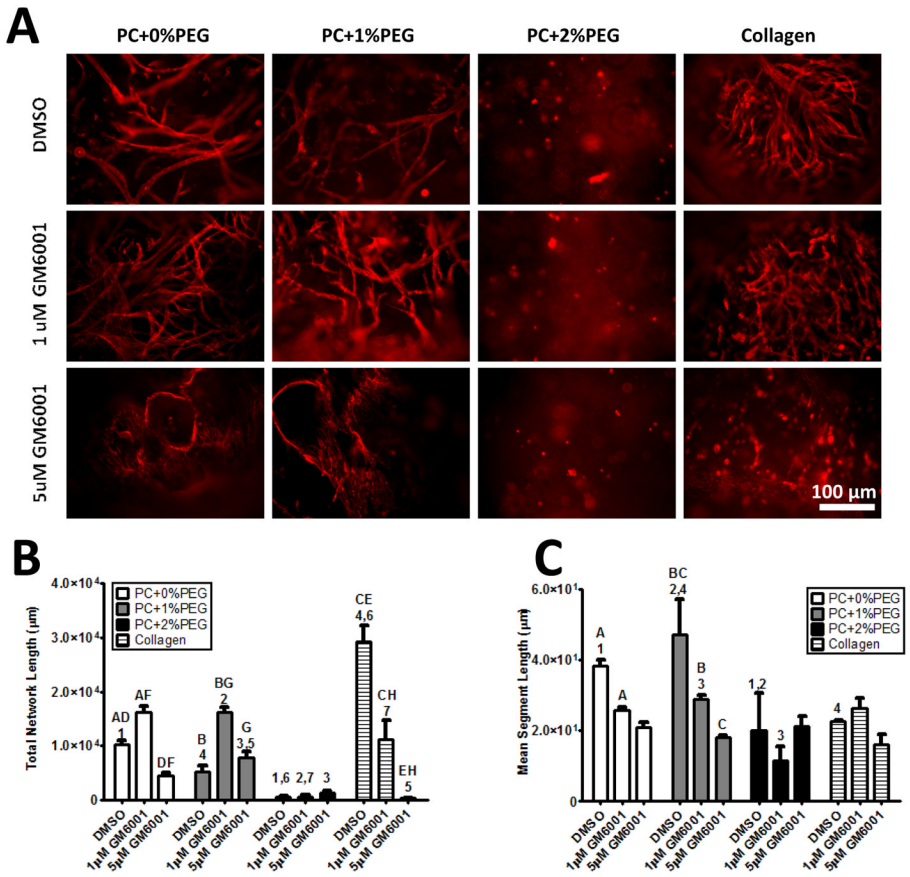

Figure 5. MMP inhibition prevents EC organization in PEG-collagen hydrogels

A) EC invasion and organization were inhibited by addition of 5 μM GM6001 in the PC +0%PEG and PC+1%PEG materials. EC survival in the PC+2%PEG condition was limited. Red staining is for CD31+ cells. B) Quantification of network morphology revealed significant increases in total network lengths in the presence of low dose GM6001 (1 μM) in PC+0%PEG and PC+1%PEG owing to a larger number of EC structures. Higher doses (5 μM) significantly reduced network lengths in PC+0%PEG. Both doses reduced total network lengths in collagen gel controls. C) Quantification of mean segment lengths showed reductions in PC+0%PEG and PC+1%PEG gels with both doses of inhibitor. Matched symbols denote statistical significance ($P < 0.01$).